

# Numerical Modelling for Investigations on Influences of Spoiler Relating to Fluid Flow over a Cavity Concerning Pressure Field and Sound Pressure Level Using LES Approach

Dr. Nirmal Kumar Kund

Associate Professor, Department of Production Engineering, Veer Surendra Sai University of Technology, Burla 768018, India

**Abstract** – The current research involves the establishment of a suitable numerical model pertaining to the supersonic flow over a 3D cavity having a length-to-depth ratio of 2. The Mach number of the supersonic free-stream is 2 and the Reynolds number of the flow is  $10^5$ . The numerical simulations have been performed by using Large Eddy Simulation (LES) approach. The Smagorinsky model is employed for this study. The results have been presented in the form of pressure field and overall sound pressure level. As observed, the feedback loop mechanism explains the nature of flow field of the cavity very well. Large pressure fluctuations are also observed inside the cavity without spoiler. However, the suppression of the pressure oscillations inside the cavity is achieved by employing a spoiler in the form of one-fourth of a cylinder at the leading edge of the cavity. The pressure less than the free-stream pressure is achieved inside the cavity. With the use of the spoiler, the overall sound pressure level is also reduced to some extent. Correspondingly, the sound pressure level is reduced by nearly 12 dB at the front wall and about 7 dB at the aft wall of the cavity. The changes in the flow feature of the cavity employing the spoiler is also investigated. In overall, the comparisons between the results of the cavity flows with and without the use of the spoiler is also done.

**Index Terms** – Numerical, Cavity, Spoiler, LES, Pressure Field, OASPL

## 1. INTRODUCTION

The presence of irregular structures or unsteady flow leads to huge aerodynamic noise resulting in aero-acoustic resonance. It is because of the aerodynamic forces acting on the surface of the moving objects. This is observed in our day-to-day life like exhaust pipes, vacuum cleaners, ventilation systems, fans etc. Noise created by a flow is the most vital issue in numerous engineering practices concerning surface transport, aviation and marine applications such as defence vehicles, submarines, aircrafts, automobiles, fighter planes, etc. It results in uneasiness to humans and also disturb the furtiveness of tasks/concerts.

Airframe noise is caused by large pressure fluctuations inside the gear box. It is a significant constituent of overall noise, mainly while landing and take-off. Noise from landing gear, flaps, slats etc. are considered as airframe noise. One of the most important airframe noises is the cavity noise. It generated from open wheel wells after the undercarriage while landing. The weapon bays in the military aircrafts involve oscillations induced by the flow, which can stimulate the vibrational modes of the structure of the aircraft. At low Mach numbers for surface transport, the automotive sectors are worried with the noises caused from the door gaps, side mirrors, and the open sun roof. These noises creations also influence the ease in the car.

The door gaps, wheel wells and weapon bays can be modelled as rectangular cavities and the composed flow beyond the cavity can be considered to be even. Although the rectangular cavity is simple in shape, it is rich in different dynamic and acoustic phenomena, likely covered by an aeroacoustic feedback loop depending on the shape/size of the cavity as well as the flow situations. Severe tone noises may be generated owing to the vortex shredding at the upstream edge of the cavity, while the flow past a cavity.

## 2. LITERATURE REVIEW

The flow-induced pressure oscillations in shallow cavities are studied by Heller et al. [1]. The investigations on the tones and pressure oscillations induced by flow over rectangular cavities are carried out by Tam and Block [2]. Mach 0.6 to 3.0 flows over rectangular cavities are performed by Kaufman et al. [3]. The high resolution schemes are used by Sweby [4] in applying flux limiters on hyperbolic conservation laws. The numerical simulation on supersonic flow over a 3D cavity are reported by Rizzetta [5]. The very fundamentals of computational fluid dynamics is demonstrated by Anderson and Wendt [6]. The achievements and challenges of large-eddy simulation are described by Piomelli [7]. The numerical simulations of fluidic control for transonic cavity flows are carried out by Hamed et al. [8]. The LES studies on feedback-

loop mechanism of supersonic open cavity flows are conducted by Li et al. [9]. A validation study on unsteady RANS computations of supersonic flow over 2D cavity is done by Vijayakrishnan [10]. The lid-driven cavity flows of viscoelastic liquids are very well illustrated by Sousa et al. [11]. The experimental investigations on double-cavity flows are described by Tuerke et al. [12]. It is observed that a broad study on cavity flow has been done both experimentally and computationally for enhancing the aerodynamic efficiency. Nevertheless, apart from its prominence, the complicated flow physics of flow past a cavity has captivated the researchers around the world for more investigations and still remains to be a thrust field of investigation.

Although, so many experiments have been performed to suppress the pressure oscillations inside the cavity, however, some are not equally effective for all flow conditions. The performance of the control devices are significantly affected by the Mach number. Control devices need to be designed so that they operate over a broad range of Mach numbers. The incoming boundary layer is also another important factor which controls the performance of the control devices. Keeping this standpoint in focus, the purpose of this research is to study the flow phenomenon in a three-dimensional open cavity supersonic flow. Also, the suppression of cavity oscillations by passive method has been studied by employing spoiler at the leading edge of the cavity. The comparison between the open cavity flows with and without the use of spoiler has also been done. In overall, the present investigations relate to the development of a 3D numerical model for comparative simulation predictions of the open cavity flows in terms of pressure field and overall sound pressure level (OASPL) with and without the use of the spoilers.

### 3. DESCRIPTION OF PHYSICAL PROBLEM

Supersonic flow past a three-dimensional cavity is studied numerically. The streamwise length, depth and spanwise length of the cavity are 20 mm, 10 mm, and 10 mm, respectively. The length-to-depth ratio ( $L/D$ ) for the cavity is 2. The width-to-depth ratio ( $W/D$ ) is 1. The cavity is three-dimensional with streamwise length-to-spanwise length ratio ( $L/W$ )  $> 1$ . In addition, the Mach number of the free-stream along with the Reynolds number based on the cavity depth are taken as 2 and  $10^5$ , respectively, for setting the inflow conditions.

#### 3.1. Geometric Model

The computational domain of the cavity with the spoiler is shown in figure 1. The size of this domain, as stated previously, is  $2D \times D \times D$  (length  $\times$  depth  $\times$  width). The spoiler at the cavity leading edge has a dimension of  $0.6D$ . One-fourth part of a cylinder has been used for the shape of the spoiler. The domain is three-dimensional with  $L/W > 1$ .

The upper boundary is at a distance of  $4D$  above the cavity to ensure that no reflected shock affects the flow features inside the cavity.

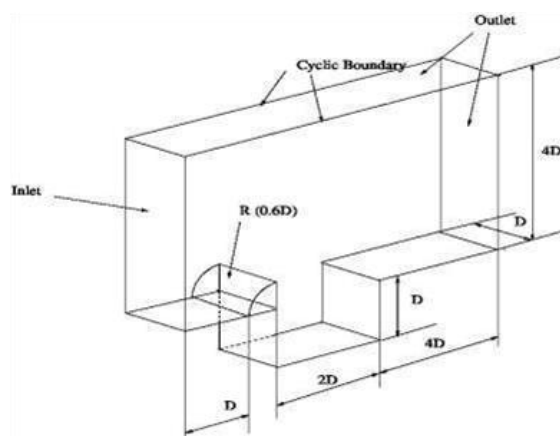


Fig 1. Computational domain of cavity with spoiler

#### 3.2. Initial and Boundary Conditions

The initial conditions for the cavity involving supersonic flow are Mach number = 2 with  $P_\infty = 101.325$  kPa and  $T_\infty = 300$  K at the inlet, Reynolds number of the flow being  $10^5$ , based on the cavity depth.

No-slip adiabatic wall boundary conditions is applied at the wall boundaries. Zero-gradient condition is applied at all the outflow boundaries. Periodical boundary condition is applied in the spanwise direction of the cavity. No-slip adiabatic wall boundary condition is employed for the spoiler.

### 4. MATHEMATICAL FORMULATION

#### 4.1. Generalized governing transport equations

The 3D compressible Navier-Stokes equations are the governing equations which comprise the continuity equation (1), the momentum equation (2), and the energy equation (3) which are as mentioned below:

$$\frac{\partial \rho}{\partial t} + \nabla \cdot (\rho \mathbf{U}) = 0 \quad (1)$$

$$\frac{\partial (\rho \mathbf{U})}{\partial t} + \nabla \cdot (\rho \mathbf{U} \cdot \mathbf{U}) - \nabla \cdot \nabla (\mu \mathbf{U}) = -\nabla p \quad (2)$$

$$\frac{\partial (\rho e)}{\partial t} + \nabla \cdot (\rho e \mathbf{U}) - \nabla \cdot \nabla (\mu e) = -p(\nabla \cdot \mathbf{U}) + \mu \left[ \frac{1}{2} (\nabla \mathbf{U} + \nabla \mathbf{U}^T) \right]^2 \quad (3)$$

Where,

$$\mathbf{U} = \text{velocity vector} = u\hat{i} + v\hat{j} + w\hat{k}$$

$$\frac{1}{2} (\nabla \mathbf{U} + \nabla \mathbf{U}^T) = \text{strain rate tensor.}$$

The equations (1), (2) and (3) symbolise the conservation form of the Navier-Stokes equations. The conservation form of these governing equations are reached from a flow model fixed in space [6]. The stated equations are relevant to viscous flow, except that the mass diffusion is not involved.

It is supposed, in aerodynamics, that the gas is a perfect gas. The equation of state for a perfect gas is,  $p = \rho RT$  (4)

Where,  $R$  = specific gas constant =  $C_p - C_v$  (5)

For a calorically perfect gas (constant specific heats), the caloric equation of state is,

$e$  = internal energy per unit mass =  $C_v T$  (6)

#### 4.2. LES Turbulence Modelling

The turbulent flows may be simulated applying three different methods: Reynolds-Averaged Navier-Stokes equations (RANS), direct numerical simulation (DNS), and large eddy simulation (LES). Direct numerical simulation has high computational necessities. DNS resolves all the scales of motion and for this it desires a number of grid points proportional to  $(Re)^{9/4}$  and computational scales' cost is proportional to  $(Re)^3$  [7].

In the current investigation, behaviours of the turbulent flow field have been simulated applying LES as it is suitable for unsteady complex flows and noise induced flows. LES computes the large resolved scales and also models the smallest scales. The turbulence model is incorporated by dividing the time and space varying flow parameters into two components, the resolved one  $\bar{f}$  and  $f'$ , the unresolved portion:

$$(x, t) = \bar{f}(x, t) + f'(x, t) \quad (7)$$

LES uses a filtering operation to separate these resolved scales from the unresolved scales. The filtered parameter is represented by an over bar [7]. The top-hat filter smooth both the fluctuations of the large-scale as well as those of small scales. The filtering operation whenever introduced to the Navier-Stokes equation, it results in:

$$\frac{\partial \bar{p}}{\partial t} + \nabla \cdot (\bar{\rho} \bar{U}) = 0 \quad (8)$$

$$\frac{\partial (\bar{\rho} \bar{U})}{\partial t} + \nabla \cdot (\bar{\rho} \bar{U} \cdot \bar{U}) - \nabla \cdot \nabla (\bar{\mu} \bar{U}) = -\nabla \bar{p} \quad (9)$$

$$\frac{\partial (\bar{\rho} \bar{e})}{\partial t} + \nabla \cdot (\bar{\rho} \bar{U} \bar{e}) - \nabla \cdot \nabla (\bar{\mu} \bar{e}) = -\bar{p} (\nabla \cdot \bar{U}) + \mu \left[ \frac{1}{2} (\nabla \bar{U} + \nabla \bar{U}^T) \right]^2 \quad (10)$$

Nevertheless, the dissipative scales of motion are rectified poorly by LES. In a turbulent flow, the energy from the large resolved structures are passed on to the smaller unresolved structures by an inertial and an effective inviscid mechanism. This is called as energy cascade. Therefore, LES employs a

sub-grid scale model to mimic the drain pertaining to this energy cascade. Most of these models are eddy viscosity models connecting the subgrid-scale stresses ( $\tau_{ij}$ ) and the resolved-scale rate of strain-tensor ( $\bar{S}_{ij}$ ),

$$\tau_{ij} - (\delta_{ij}/3) = -2\nu_T \bar{S}_{ij} \quad (11)$$

Where,  $\bar{S}_{ij}$  is the resolved-scale rate of strain tensor =  $(\partial \bar{u}_i / \partial x_j + \partial \bar{u}_j / \partial x_i) / 2$ .

In most of the circumstances it is supposed that all the energy received by the unresolved-scales are dissipated instantly. This is the equilibrium assumption, i.e., the small-scales are in equilibrium [7]. This simplifies the problem to a great extent and an algebraic model is found for the eddy viscosity:

$$\mu_{sgs} = \rho C \Delta^2 |\bar{S}| |\bar{S}|, |\bar{S}| = (2\bar{S}_{ij} \bar{S}_{ij})^{1/2} \quad (12)$$

Here,  $\Delta$  is the grid size and is generally considered to be the cube root of the cell volume [7]. This model is termed as the Smagorinsky model and  $C$  is the Smagorinsky coefficient. In the current investigation, its value has been considered to be 0.2.

## 5. NUMERICAL PROCEDURES

### 5.1. Numerical scheme and solution algorithm

The 3D compressible Navier-Stokes governing transport equations are discretized over an outline concerning finite volume method (FVM) through the SIMPLER algorithm. Here, the turbulent model utilized for large eddy simulation is Smagorinsky model, on account of its minimalism. The spatial derivatives like Laplacian and convective terms are computed by second order scheme based on Gauss theorem. Furthermore, the viscous terms are calculated by second order scheme. Additionally, the implicit second order scheme is utilized for time integration. The numerical fluxes are calculated by using Sweby limiter in central differencing (CD) scheme, which is a total variation diminishing (TVD) scheme. The central differencing (CD) is an unbounded second order scheme, while, the total variation diminishing (TVD) is a limited linear scheme. The developed solver is utilized to predict flow behaviours of the related flow variables pertaining to supersonic flow over an open cavity.

### 5.2. Choice of grid size, time step and convergence criteria

The computational domain is again decomposed into upper cavity and inside cavity region as illustrated in figure 2. The grid is refined at the regions near to the wall (where very high gradient is expected) to determine the behaviour of shear layer satisfactorily. A comprehensive grid-independence test is performed to establish a suitable spatial discretization, and the levels of iteration convergence criteria to be used. As an outcome of this test, the optimum number of grid points used for the final simulation, in the upper cavity region as  $360 \times 150 \times 1$  and those of in the inside

cavity region as  $200 \times 150 \times 1$ . The grid spacing at the leading edge of the cavity denoted as  $\Delta X^+$ ,  $\Delta Y^+$  and  $\Delta Z^+$  being 5.0, 12.5, and 1.0, respectively. However, the total number of grid points is 81000 for this cavity. Corresponding time step chosen in the numerical simulation is  $10^{-6}$  seconds. Even though, it is tested with smaller grids of 128000 in numbers, it is witnessed that a finer grid structure does not change the results considerably.

The convergence in inner iterations is confirmed only when the condition  $\left| \frac{\varphi - \varphi_{old}}{\varphi_{max}} \right| \leq 10^{-4}$  is fulfilled concurrently for all variables, where  $\varphi$  represents the field variable at a grid point at the current iteration level,  $\varphi_{old}$  stands for the corresponding value at the previous iteration level, and  $\varphi_{max}$  is the maximum value of the variable at the current iteration level in the whole domain.

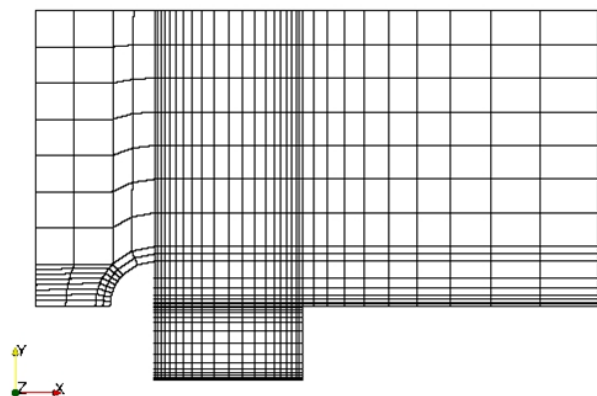


Fig 2. Computational grid of cavity with spoiler in X-Y Plane

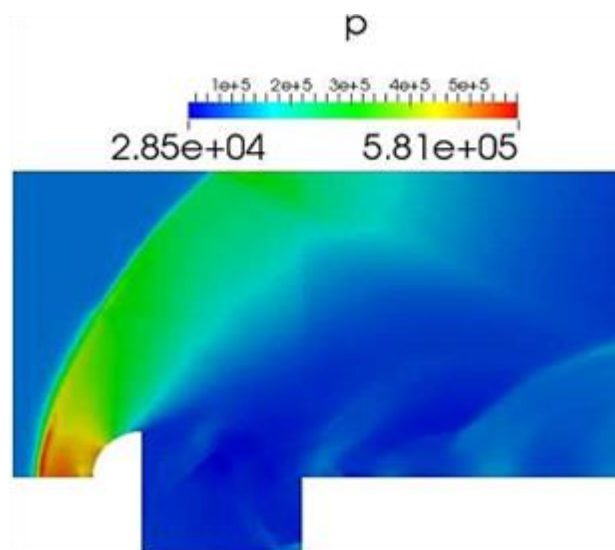
## 6. RESULTS AND DISCUSSIONS

The pressure fluctuations need to be reduced inside the cavity. Moreover, the noise produced due to the flow past a cavity need to be reduced. This can be achieved by employing a spoiler at the leading edge of the cavity. The spoiler employed in the present research is one-fourth part of a cylinder.

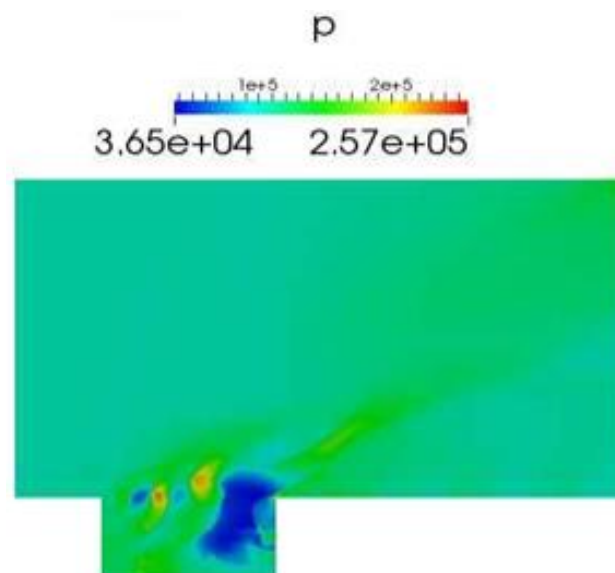
### 6.1. Comparisons of pressure distributions with and without spoiler

The pressure fields, at an instant of time  $t = 0.2$  sec, for supersonic flow over a cavity with and without the use of spoiler are illustrated in the figure 3. The flow feature of the cavity with spoiler is different from that of the cavity without spoiler. The difference in the flow fields may easily be observed from the pressure fields. One shedding vortex is seen in the cavity with spoiler in contrast to two shedding vortices observed in the cavity without spoiler. The pressure inside the cavity is less than the free stream pressure for most of the time. The recirculation regions for

both the cavities are quite different from each other. A shock is seen to be reflected from the upper boundary, however, it does not have any effect on the flow field inside the cavity. The pressure fields, at another instant of time  $t = 0.4$  sec, are also demonstrated in the figure 4. The comparisons of the flow features can also be made from both the stated figures realized at two different instants of times.

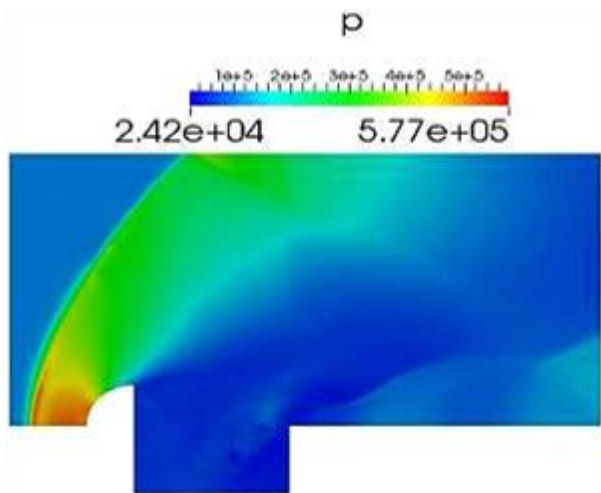


(a) With Spoiler

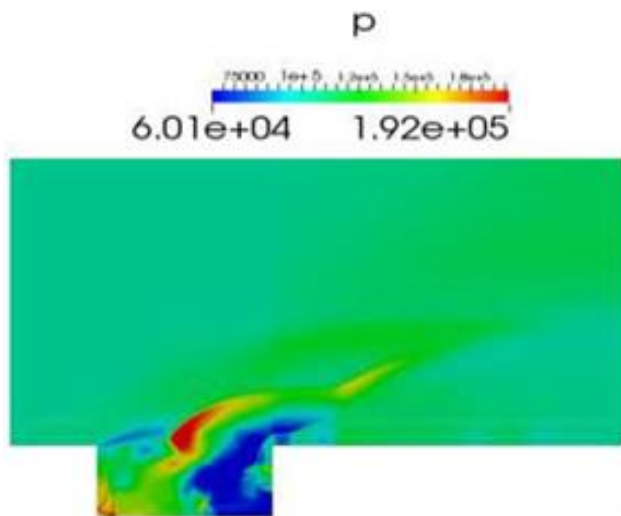


(b) Without Spoiler

Fig 3. Pressure field at time,  $t = 0.2$  sec with and without the use of spoiler



(a) With Spoiler



(b) Without Spoiler

Fig 4. Pressure field at time,  $t = 0.4$  sec with and without the use of spoiler

### 6.2. Comparison of overall sound pressure level (OASPL) with and without use of spoiler

The comparison of the OASPL (Overall Sound Pressure Level) distributions along the bottom wall of the cavity has also been done. The OASPL is represented as:

$$OASPL = 10 \log_{10}(\overline{p_d^2}/q^2) \tag{13}$$

Where,

$$\overline{p_d^2} = \frac{1}{t_f - t_i} \int_{t_i}^{t_f} (p - \bar{p})^2 dt \tag{14}$$

$q$  is the acoustic sound reference level with a value equal to  $2 \times 10^{-5}$  Pa

$\bar{p}$  is the time-averaged static pressure

$t_f$  and  $t_i$  are the initial and final times, respectively

The OASPL distribution of cavity with spoiler has been compared with that of without the use of spoiler. The comparison of both the stated cases are shown in the figure 5. It is observed that the OASPL is reduced by nearly 7 dB at the aft wall of the cavity and also reduced by nearly 12 dB at the front wall of the cavity.

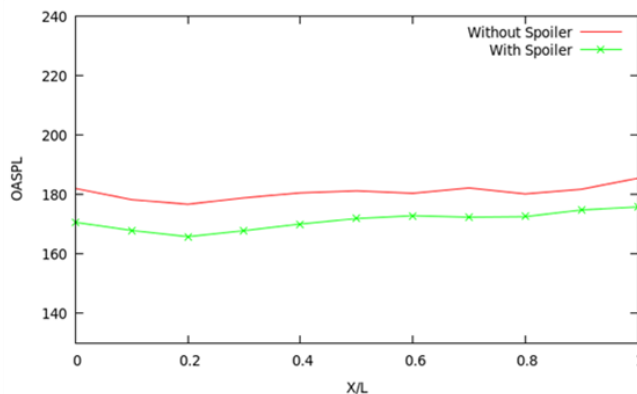


Fig 5. OASPL distribution at the centreline of the bottom wall of the cavity with and without the use of spoiler

### 7. CONCLUSIONS

In the present work, the numerical simulation has been performed for supersonic flow over open cavity with and without the use of spoiler. The cavity has length-to-depth ratio of 2 and Mach number of the free-stream is 2.0. The simulation is carried by using LES based Smagorinsky model. The results are presented in the form of both cavity flow-field analysis and the aeroacoustic analysis represented by the overall sound pressure level. The LES model is able to predict all the main flow features of the cavity. The overall sound pressure level of the cavity with spoiler is compared with that of without the spoiler. There is qualitative agreement between the two. However, with the use of spoiler, the sound pressure level is decreased by around 7 dB at the aft wall and also reduced by nearly 12 dB at the front wall of the cavity. The trends of results for both the cavity are similar and hence are comparable. The pressure inside the cavity is also reduced and the values less than the free-stream pressure is achieved. In overall, in this research, a 3D model is developed for a cavity and a spoiler is employed at its leading edge to investigate the flow features and to suppress the pressure fluctuations inside the cavity. In addition, the overall sound pressure level is also observed to be suppressed.

### REFERENCES

[1] Heller, H. H., Holmes, D. G., & Covert, E. E. (1971). Flow-induced pressure oscillations in shallow cavities. Journal of sound and Vibration, 18(4), 545-553.

- [2] Tam, C. K., & Block, P. J. (1978). On the tones and pressure oscillations induced by flow over rectangular cavities. *Journal of Fluid Mechanics*, 89(02), 373-399.
- [3] Kaufman, I. I., Louis, G., Maciulaitis, A., & Clark, R. L. (1983). Mach 0.6 to 3.0 flows over rectangular cavities (No. AFWAL-TR-82-3112). Air force wright aeronautical labs wright-patterson AFB, OH.
- [4] Sweby, P. K. (1984). High resolution schemes using flux limiters for hyperbolic conservation laws. *SIAM journal on numerical analysis*, 21(5), 995-1011.
- [5] Rizzetta, D. P. (1988). Numerical simulation of supersonic flow over a three-dimensional cavity. *AIAA journal*, 26(7), 799-807.
- [6] Anderson, J. D., & Wendt, J. F. (1995). *Computational fluid dynamics* (Vol. 206). New York: McGraw-Hill.
- [7] Piomelli, U. (1999). Large-eddy simulation: achievements and challenges. *Progress in Aerospace Sciences*, 35(4), 335-362.
- [8] Hamed, A., Das, K., & Basu, D. (2004). Numerical simulations of fluidic control for transonic cavity flows. *AIAA Paper*, 429, 2004.
- [9] Li, W., Nonomura, T., Oyama, A., & Fujii, K. (2010). LES Study of Feedback-loop Mechanism of Supersonic Open Cavity Flows. *AIAA paper*, 5112, 2010.
- [10] Vijaykrishnan, K. (2014) Unsteady RANS computations of supersonic flow over two dimensional cavity using OpenFOAM-A validation study. *AIAA* 2014.
- [11] Sousa, R. G., et al. (2016). Lid-driven cavity flow of viscoelastic liquids. *Journal of Non-Newtonian Fluid Mechanics*, 234, 129-138, 2016.
- [12] Tuerke, F., Pastur, L. R., Sciamarella, D., Lusseyran, F., & Artana, G. (2017). Experimental study of double-cavity flow. *Experiments in Fluids*, 76, 2017.